

Supplementary material for:

Synthesis and studies of the inhibitory effect of hydroxylated phenylpropanoids and biphenols derivatives on tyrosinase and laccase enzymes

Maria Antonietta Dettori^{1,#}, Davide Fabbri^{1,#}, Alessandro Dessì¹, Roberto Dallochio¹, Paola Carta¹, Claudia Honisch^{2,3}, Paolo Ruzza^{2,3}, Donatella Farina⁴, Rossana Migheli⁴, Pier Andrea Serra⁴, Roberto A. Pantaleoni^{5,6}, Xenia Fois⁶, Gaia Rocchitta^{4,*}, Giovanna Delogu^{1,*}

- 1 Istituto di Chimica Biomolecolare, Consiglio Nazionale Ricerche, Sassari, Italy. M.A.D. mariaantonieta.dettori@cnr.it; D.F. davidegaetano.fabbri@cnr.it; A.D. alessandro.dessi@cnr.it; R.D. robertonico.dallochio@cnr.it; P.C. paola.carta@cnr.it; G.D. giovanna.delogu@icb.cnr.it
- 2 Dipartimento di Scienze Chimiche, Università degli Studi di Padova, Padova, Italy. C.H. claudia.honisch@phd.unipd.it
- 3 Istituto di Chimica Biomolecolare, Consiglio Nazionale Ricerche, Padova, Italy. C.H. claudia.honisch@unipd.it; P.R. paolo.ruzza@cnr.it.
- 4 Dipartimento di Scienze Mediche, Chirurgiche e Sperimentali, Università degli Studi, Sassari, Italy. D.F. donatellafarina@tiscali.it; R.M. rmigheli@uniss.it; P.A.S. paserra@uniss.it; G.R. grocchitta@uniss.it
- 5 Istituto di Ricerca sugli Ecosistemi Terrestri, Consiglio Nazionale Ricerche, Sassari, Italy. R.P. roberto.pantaleoni@iret.cnr.it; X.F. xeniafois@hotmail.it
- 6 Dipartimento di Agraria, Università degli Studi, Sassari, Italy. R.A.P. pantaleo@uniss.it;

M.A.D. and D.F. contributed equally to this work.

* Correspondence: +39 079228526, grocchitta@uniss.it (G.R.); +39 079 2841220, giovanna.delogu@icb.cnr.it (G.D.)

Table of the contents

1.1 Chemistry synthesis of compounds 7 and 12-17	S2
1.2 Spectrophotometric assay of tyrosine and dopamine: Figures S1 and S2	S5
1.3 Electrochemical assays: biosensor calibration and inhibition protocols	S6
1.4 Viability and oxidative stress assays	S7
1.5 Kinetic parameters, Lineweaver–Burk plot and viability graphics of compounds 7-20: Table S1 and Figures S3-S16	S8
1.6 Representative plot of IC ₅₀ calculation for compound 20	S23
1.7 Computational studies of compounds DFB, 1 and 20: Tables S2 and S3	S24
1.8 References	S25

1.1 Chemistry

Unless otherwise noted, starting materials and reagents were obtained from commercial suppliers and were used without further purification. Melting points were determined on a Büchi 530 apparatus and are uncorrected. All ^1H NMR and ^{13}C NMR spectra were recorded in CDCl_3 (if not otherwise indicated) solution with a Varian VXR 5000 spectrometer at 399.94 MHz and 75.42 MHz respectively. Chemical shifts are given in ppm (δ); multiplicities are indicated by s (singlet), d (doublet), t (triplet), q (quartet), m (multiplet), td (triplet of doublets) or dd (doublet of doublets). Elemental analyses were performed using an elemental analyser Perkin-Elmer model 240 C. Acetone was freshly distilled from CaCl_2 . Flash chromatography was carried out with silica gel 60 (230-400 mesh, Kiesgel, EM Reagents) eluting with appropriate solution in the stated v:v proportions. Analytical thin-layer chromatography (TLC) was performed with 0.25 mm thick silica gel plates (Polygram® Sil G/UV254, Macherey-Nagel). All reactions were monitored by TLC performed on 0.2 mm thick silica gel plates (60 F254 Merck). The purity of all new compounds was judged to be >98% by ^1H NMR spectral determination.

Compounds **8** (*E*)-4-(4-hydroxy-3-methoxyphenyl)but-3-en-2-one, **9** 4-(3,4-dihydroxyphenyl)butan-2-one, **10** (*E*)-3-(4-hydroxy-3-methoxyphenyl)-1-phenylprop-2-en-1-one and **11** (*E*)-1-(3,4-dimethoxyphenyl)-3-(4-hydroxy-3-methoxyphenyl)prop-2-en-1-one were prepared according to the literature procedures [1-4].

(E)-4-(2,4-dihydroxyphenyl)but-3-en-2-one **7**

To a stirred solution of 2,4-dihydroxybenzaldehyde (3.0 g, 21.7 mmol) in acetone (50 mL) at room temperature and under N_2 , an aqueous solution (1 N) of NaOH (80 mL, 80 mmol) was added dropwise. The mixture was stirred at 50°C for 12 h. The solvent was roto-evaporated, water and hydrochloridric acid (10% solution) were cautiously added. The heterogeneous solution was extracted with ether, dried over anhydrous sodium sulphate and evaporated. The crude product was purified by flash chromatography using a 1:1 mixture of petroleum ether: ethyl acetate as eluent to give compound **7** as dark solid (2.3 g, 60%): mp $119\text{--}121^\circ\text{C}$ (lit.[5] $118\text{--}120^\circ\text{C}$); ^1H -NMR (CD_3COCD_3) δ 2.25 (s, 3H), 6.41 (dd, $J = 2.0, 8.4$ Hz, Ar, 1H), 6.47 (d, $J = 2.0$ Hz, Ar, 1H), 6.67 (d, $J = 16.4$ Hz, 1H), 7.48 (d, $J = 8.4$ Hz, Ar, 1H), 7.82 (d, $J = 16.4$ Hz, Ar, 1H); ^{13}C -NMR (CD_3COCD_3) δ 26.34, 102.69, 108.14, 113.73, 123.88, 129.95, 138.41, 158.32, 160.92, 197.07. Anal. Calcd. for $\text{C}_{10}\text{H}_{12}\text{O}_3$: C, 66.65; H, 6.71 Found: C, 66.72; H, 6.53.

(E)-1-(3,4-dimethoxyphenyl)-3-(4-hydroxy-3-methoxyphenyl)prop-2-en-1-one **12**.

To a stirred solution of KOH (1.14 g, 20.32 mmol) in water (4 mL) was added dropwise a solution of 3,4-dimethoxybenzaldehyde (1.70 g, 10.23 mmol) and apocynin (1.70 g, 10.23 mmol) in methanol (20 mL). The reaction mixture was stirred at room temperature for 96 h under N_2 . The mixture was poured into ice-water (10 mL), adjusted to pH 3–4 with hydrochloridric acid (10% solution), and then extracted with ethyl acetate. The organic layer was successively washed with water and saturated brine, dried over anhydrous sodium sulphate and purified by flash chromatography using a 2:1 mixture of ethyl acetate:petroleum as eluent to give **12** as a yellow solid (2.72 g, 85%): mp = $110\text{--}112^\circ\text{C}$; ^1H NMR δ 3.92 (s, 3H), 3.95 (s, 3H), 3.97 (s, 3H), 6.21 (bs, 1H), 6.88 (d, $J = 8.0$ Hz, Ar, 1H), 6.98 (d, $J = 8.4$ Hz, Ar, 1H), 7.15 (d, $J = 2$ Hz, Ar, 1H), 7.28 (dd, $J = 1.6, 8$ Hz, Ar, 1H), 7.41 (d, $J = 15.6$ Hz, 1H), 7.62–7.70 (series of m, Ar, 2H), 7.75 (d, $J = 15.6$ Hz, 1H); ^{13}C NMR δ 55.97, 55.99, 56.12, 110.09, 110.48, 111.09, 113.71, 119.54, 122.95, 123.52, 128.03, 131.22, 144.15, 146.88, 149.21, 150.23, 151.25, 188.58; Anal. Calcd. for $\text{C}_{18}\text{H}_{18}\text{O}_5$: C, 68.78; H, 5.77; Found: C, 68.69; H, 5.56.

(*E*)-4-(4-hydroxy-3-methoxyphenyl)-1-((2*S*,3*R*,4*R*,5*S*,6*R*)-3,4,5-trihydroxy-6-(hydroxymethyl)tetrahydro-2H-pyran-2-yl)but-3-en-2-one **13**.

Compound **23** (0.30 g, 0.57 mmol) was stirred in sodium methoxide/methanol solution (0.006 g, 0.11 mmol in 10 mL) for 10 min. The reaction mixture was neutralized using a Dowex Marathon C (H⁺ form) resin, filtrated and concentrated *in vacuo* to obtain **13** as a brown solid. (0.19 g, 94%): mp = 54-55°C; [α]_D²⁰ 11.7 (c 0.5, MeOH); ¹H NMR (CD₃OD) δ 2.86 (dd, *J* = 9.2, 16.0 Hz, 1H), 3.10 (dd, *J* = 2.8, 16.0 Hz, 1H), 3.14-3.41 (series of m, 4H), 3.62 (dd, *J* = 5.2, 12.4 Hz, 1H), 3.72-3.79 (series of m, 2H), 3.88 (s, 3H), 6.73 (d, *J* = 16.4 Hz, 1H), 6.81 (d, *J* = 8.0 Hz, Ar, 1H), 7.12 (dd, *J* = 2.0, 8.4 Hz, Ar, 1H), 7.21 (d, *J* = 2.0 Hz, Ar, 1H), 7.59 (d, *J* = 16.4 Hz, 1H); ¹³C NMR δ (CD₃OD) 42.80, 55.06, 61.35, 70.25, 73.76, 76.16, 78.31, 80.16, 110.59, 115.16, 123.11, 123.34, 126.42, 144.51, 147.98, 149.54, 199.88; Anal. Calcd. for C₁₇H₂₂O₈: C, 57.62; H, 6.26; Found: C, 57.70; H, 6.31.

(2*E*,2'*E*)-1,1'-(5,5',6,6'-tetramethoxy-[1,1'-biphenyl]-3,3'-diyl)bis(3-(4-hydroxy-3-methoxyphenyl)prop-2-en-1-one) **14**.

To a stirred solution of KOH (6.20 g, 110.51 mmol) in water (6 mL) cooled to 0 °C in an ice bath was added dropwise a solution of tetrahydropyranyl vanillin acetal [6] (1.16 g, 4.91 mmol) and OMe-dehydrodiapocynin [7] (0.44 g, 1.22 mmol) in methanol (30 mL). The reaction mixture was kept at 0 °C for 3 h, and then at room temperature for 12 h, under N₂. *p*-Toluenesulfonic acid (0.02 g, 0.12 mmol) was added and the solution was stirred for 2 h. The mixture was poured into ice-water (10 mL), adjusted to pH 3-4 with hydrochloridric acid (10% solution), and then extracted with ethyl acetate. The organic layer was successively washed with water and saturated brine, dried over anhydrous sodium sulphate and purified by flash chromatography using a 1:1 mixture of ethyl acetate:petroleum as eluent to give **14** as a yellow solid (0.61 g, 80%): mp = 209-210°C; ¹H NMR δ 3.77 (s, 6H), 3.92 (s, 6H), 4.01 (s, 6H), 6.01 (bs, 2H), 6.92 (d, *J* = 8.0 Hz, Ar, 2H), 7.11 (d, *J* = 2.0 Hz, Ar, 2H), 7.19 (dd, *J* = 2.0, 8.4 Hz, Ar, 2H), 7.35 (d, *J* = 16.0 Hz, 2H) 7.61 (d, *J* = 2.4 Hz, Ar, 2H), 7.71 (d, *J* = 2.4 Hz, Ar, 2H), 7.79 (d, *J* = 16.0 Hz, 2H); ¹³C NMR δ 56.08, 56.09, 60.91, 110.07, 111.67, 114.83, 118.96, 123.51, 124.21, 127.43, 131.47, 133.88, 145.17, 146.78, 148.31, 150.87, 153.03, 188.87; Anal. Calcd. for C₃₆H₃₄O₁₀: C, 69.00; H, 5.47; Found: C, 69.18; H, 5.36.

General procedure for the synthesis of chalcones **15** and **16**

To a stirred solution of KOH (90 eq) in water (4 mL) cooled to 0 °C in an ice bath was added dropwise a solution of OMe-dehydrovanillin [8] (1 eq) and 4-hydroxy-3-methoxyacetophenone (for **15**) or 2-hydroxy-5-methoxyacetophenone (for **16**) (3 eq) in methanol (20 mL). The reaction mixture was kept at 0 °C for 3 h, and then at room temperature for 96 h, under N₂. The mixture was poured into ice-water (10 mL), adjusted to pH 3-4 with hydrochloridric acid (10% solution), and then extracted with ethyl acetate. The organic layer was successively washed with water and saturated brine, dried over anhydrous sodium sulphate and purified by flash chromatography using a 2:1 mixture of ethyl acetate:petroleum as eluent to give **15** or **16**.

(2*E*,2'*E*)-3,3'-(5,5',6,6'-tetramethoxy-[1,1'-biphenyl]-3,3'-diyl)bis(1-(4-hydroxy-3-methoxyphenyl)prop-2-en-1-one) **15**: yellow solid (70%): mp = 220-222°C; ¹H NMR δ 3.73 (s, 6H), 3.98 (s, 6H), 3.99 (s, 6H), 6.15 (bs, 2H), 6.98 (d, *J* = 8.0 Hz, Ar, 2H), 7.19 (d, *J* = 2.0 Hz, Ar, 2H), 7.20 (d, *J* = 2.0 Hz, Ar, 2H), 7.47 (d, *J* = 15.6 Hz, 2H), 7.64 (m, Ar, 4H), 7.76 (d, *J* = 15.6 Hz, 2H); ¹³C NMR δ 56.01, 56.16, 60.91, 110.42, 111.83, 113.73, 120.93, 123.45,

123.68, 130.55, 131.04, 132.48, 143.66, 146.88, 148.91, 150.33, 152.96, 188.39; Anal. Calcd. for C₃₆H₃₄O₁₀: C, 69.00; H, 5.47; Found: C, 69.09; H, 5.46.

2E,2'E-3,3'-(5,5',6,6'-tetramethoxy-[1,1'-biphenyl]-3,3'-diyl)bis(1-(2-hydroxy-5-methoxyphenyl)prop-2-en-1-one) **16**: yellow solid (55%): mp = 190-192°C; ¹H NMR δ 3.75 (s, 6H), 3.82 (s, 6H), 3.99 (s, 6H), 6.96 (d, *J* = 8.8 Hz, Ar, 2H), 7.13 (dd, *J* = 2.8, 8.8 Hz, Ar, 2H), 7.21 (d, *J* = 2.0 Hz, Ar, 2H), 7.24 (d, *J* = 2.0 Hz, Ar, 2H), 7.35 (d, *J* = 2.8 Hz, Ar, 2H), 7.51 (d, *J* = 16.0 Hz, 2H), 7.89 (d, *J* = 16.0 Hz, 2H); ¹³C NMR δ 56.06, 56.23, 60.95, 112.18, 113.42, 119.25, 119.32, 119.70, 123.40, 123.84, 130.06, 132.48, 145.33, 149.46, 151.65, 153.02, 157.84, 193.18; Anal. Calcd. for C₃₆H₃₄O₁₀: C, 69.00; H, 5.47; Found: C, 69.15; H, 5.41.

(*2E,2'E*)-diethyl 3,3'-(6,6'-dihydroxy-5,5'-dimethoxy-[1,1'-biphenyl]-3,3'-diyl)diacrylate **17**.

To a stirred solution of ferulic acid dimer [9] (1.11 g, 2.87 mmol) in absolute ethanol (10 mL) was added concentrated sulphuric acid (0.1 mL). The reaction mixture was stirred at reflux for 12 h. Water (100 mL) and dichloromethane (100 mL) were added. The organic layer was successively washed with an aqueous saturated solution of sodium bicarbonate, dried over anhydrous sodium sulphate and evaporated to obtain pure **17** as a brown solid. (1.20 g, 95%): mp = 100-102°C; ¹H NMR δ 1.33 (t, *J* = 7.2 Hz, 6H), 3.97 (s, 6H), 4.24 (q, *J* = 7.2 Hz, 4H), 6.21 (s, 2H), 6.32 (d, *J* = 15.6 Hz, 2H), 7.07 (d, *J* = 2.0 Hz, Ar, 2H), 7.14 (d, *J* = 2.0 Hz, Ar, 2H), 7.62 (d, *J* = 15.6 Hz, 2H); ¹³C NMR δ 14.34, 56.18, 60.38, 108.72, 116.19, 123.55, 124.82, 126.73, 144.49, 145.07, 147.25, 167.18; Anal. Calcd. for C₂₄H₂₆O₈: C, 65.15; H, 5.92; Found: C, 65.11; H, 5.91.

(*2R,3R,4R,5S,6S*)-2-(acetoxymethyl)-6-((*E*)-4-(4-hydroxy-3-methoxyphenyl)-2-oxobut-3-en-1-yl)tetrahydro-2H-pyran-3,4,5-triyl triacetate **23**.

To a stirred solution of tetrahydropyranyl vanillin acetal [6] (0.52 g, 2.22 mmol) and *per-O*-acetylated-β-C-glucopyranosyl ketone [10] (0.86 g, 2.22 mmol) in dichloromethane (30 mL) was added pyrrolidine (0.3 mL). The reaction mixture was stirred for 72 h, then was poured into ice-water (10 mL), adjusted to pH 3-4 with hydrochloric acid (10% solution). The organic layer was successively washed with water and saturated brine, dried over anhydrous sodium sulphate and evaporated. Methanol (30 mL) and pyridinium-*p*-toluenesulfonate (0.05g, 0.21 mmol) were added and the solution was stirred for 3 h. The mixture was evaporated to give a yellow oil that was purified by flash chromatography using a 2:5 mixture of petroleum: acetone as eluent to obtain **23** as a yellow solid (0.95 g, 82%): mp = 59-60°C; [α]_D²⁰ -10.0 (c = 0.5, CHCl₃); ¹H NMR δ 2.00 (s, 3H), 2.01 (s, 3H), 2.02 (s, 3H), 2.03 (s, 3H), 2.65 (dd, *J* = 3.2, 16 Hz, 1H), 2.99 (dd, *J* = 8.4, 16 Hz, 1H), 3.71 (dt, *J* = 2.0, 12.8 Hz, 1H), 3.94 (s, 3H), 4.03 (dd, *J* = 1.6, 12.4 Hz, 1H), 4.12 (m, 1H), 4.26 (dd, *J* = 4.8, 12.4 Hz, 1H), 4.98 (t, *J* = 9.6 Hz, 1H), 5.07 (t, *J* = 9.2 Hz, 1H), 5.22 (t, *J* = 9.6 Hz, 1H), 5.93 (bs, 1H), 6.63 (d, *J* = 16.4 Hz, 1H), 6.93 (d, *J* = 8.0 Hz, Ar, 1H), 7.05 (d, *J* = 1.6 Hz, Ar, 1H), 7.11 (dd, *J* = 1.6, 8.0 Hz, Ar, 1H), 7.49 (d, *J* = 16.4 Hz, 1H); ¹³C NMR δ 20.62, 20.64, 20.67, 20.74, 42.39, 55.97, 62.03, 68.51, 71.71, 74.19, 74.22, 75.71, 109.47, 114.85, 123.76, 124.01, 127.72, 144.02, 146.84, 148.48, 169.58, 170.03, 170.24, 170.65, 196.01; Anal. Calcd. for C₂₅H₃₀O₁₂: C, 57.47; H, 5.79; Found: C, 57.38; H, 5.76.

1.2 Spectrophotometric assay

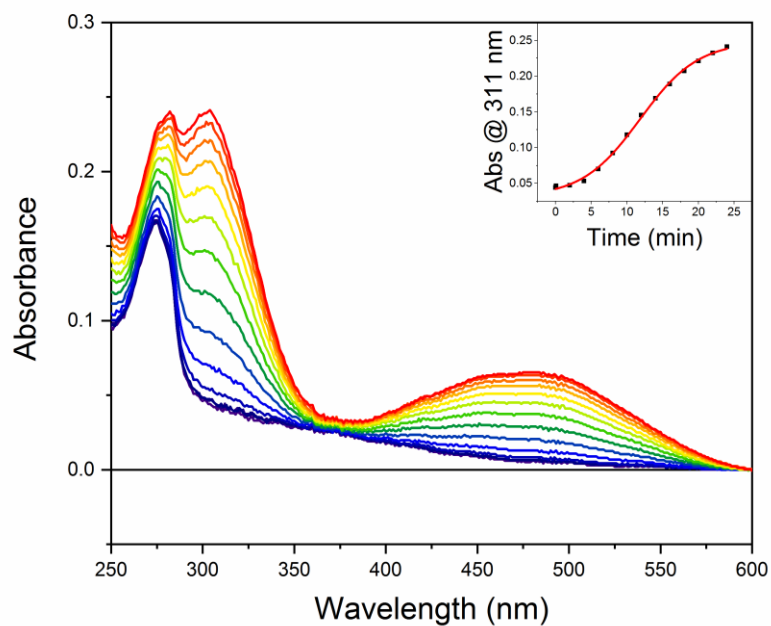


Figure S1. UV-Vis spectra of tyrosine (90 μM) in 50 mM phosphate buffer, pH 6.8, at different time after the addition of tyrosinase (83 U/mL). In the insert, the time-course of tyrosine oxidation detected at 311 nm.

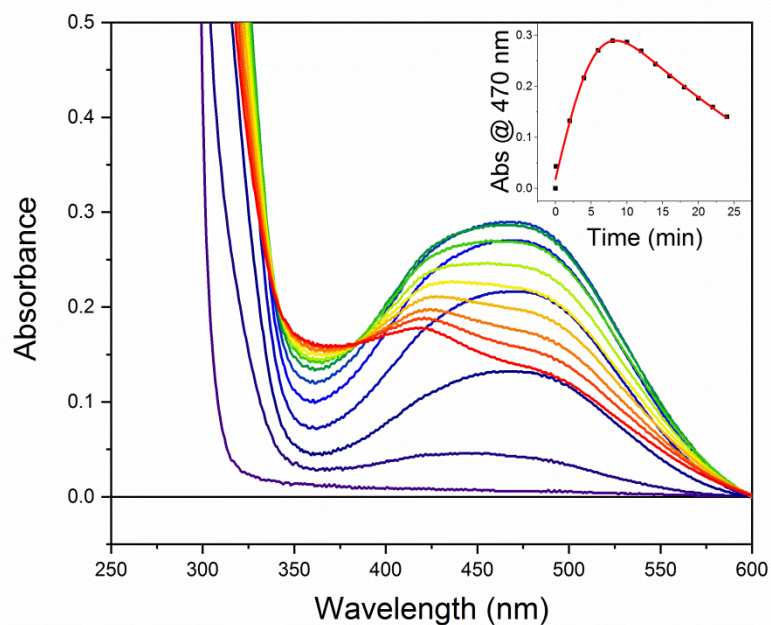


Figure S2. UV-Vis spectra of dopamine (9 μM) in 50 mM phosphate buffer, pH 6.8, at different time after the addition of tyrosinase (8.3 U/mL). In the insert, the time-course of dopamine oxidation detected at 472 nm.

1.3 Electrochemical assays: biosensor calibration and inhibition protocols

Preparation of Tyrosinase and Laccase biosensors

The biosensors were prepared starting from a Teflon™-insulated silver wire (30 mm in length; $\varnothing = 125 \mu\text{m}$), as previously described [11, 12]. Briefly, 1 mm of the silver wire was exposed and then introduced into a silica capillary cylinder (10 mm in length; I.D. $\varnothing = 180 \mu\text{m}$, Polymicro Technologies, Phoenix, AZ, USA) partly packed with graphite-loaded (55% w/w) epoxy resin. By mixing 850 mg of graphite with 500 mg of Araldite-M and 200 mg of hardener, a preliminary disc electrode of carbon-composite was fabricated ($\varnothing = 180 \mu\text{m}$; area: $2.5 \times 10^{-4} \text{ cm}^2$) by filling the silica capillary tubing with the mixture. The silver wire assured a good electrical contact. After 24 h at 40 °C, the electrode surface was cleaned using a high-speed drill (Dremel® 300) equipped with an aluminum oxide grinding wheel. On top of the electrode surface a 1 μl of Tyrosinase or Laccase solution was deposited. After the complete evaporation of water at room temperature, the biosensor was quickly dipped in the polyurethane solution in order to entrap the enzyme on the electrode surface, and after the complete evaporation of the solvent biosensors were put to stabilize in PBS pH=6.0 overnight.

Biosensor Calibration protocol

The electrochemical measurements were performed at room temperature in a classical three-electrode electrochemical cell consisting of four biosensors as working electrodes, a reference electrode (Ag/AgCl in NaCl, 3.0 M) and the auxiliary electrode (a large surface steel wire), as previously described [13, 14].

In order to characterize tyrosinase and laccase biosensors' performances, a preliminary cyclic voltammetry was performed in PBS pH=6.0, using dopamine as reference compound, so that to fix the working reduction potential of the corresponding quinone, obtained by the oxidation of the amine. In parallel, cyclic voltammeteries of inhibitors have been carried out in the same conditions as dopamine to determine any eventual overlapping of peaks in the reduction region and evaluate any possible interfering current. The voltammograms (data not shown) were obtained in a potential range from -0.5 V to +0.5 V at 100 mV s⁻¹ of scan rate.

Constant potential amperometry (CPA) was used for in-vitro calibrations and for inhibition evaluation experiments by applying a constant potential of -50 mV against an Ag/AgCl reference electrode, by means of a four-channel potentiostat (eDAQ Quadstat, e-Corder 410, eDAQ Europe, Poland) and the software Chart (v 5.5, eDAQ Europe, Poland). Thus, once the stabilization of the baseline of biosensors was reached, increasing volumes of a stock solution of dopamine 1 M were added in order to obtain different concentrations ranging from 0 to 140 mM. Biosensors were then characterized in terms of Michaelis–Menten kinetics (V_{MAX} and apparent K_{M}) as parameters taken into account to determine the possible inhibition effects of the studied molecules. Statistical differences of parameters were evaluated by means of t-test ($p < 0.05$). The statistical software GraphPad Prism v 5.02 was used for the evaluation of enzymatic kinetic parameters and IC₅₀ values and to perform t-test.

Biosensor Inhibition protocols

Two different inhibition protocols have been used. The first has been set in order to assess the IC₅₀ values of different inhibitors, as previously demonstrated. [15, 16]. Briefly, a fixed concentration of dopamine (50 μM in 10 ml of PBS pH=6.0 at a fixed potential of -50 mV vs Ag/AgCl) has been injected in the electrochemical cell. After having reached a stable baseline, known volumes of a stock solution of each inhibitor (10 mM) have been added in the cell up to the desired concentration. The second protocol has been explained in the manuscript

at 4.3. paragraph of the Materials and Methods section. For each inhibitor was built a group of biosensors (n=4) for both tyrosinase and laccase enzyme.

1.4 Viability and oxidative stress assays

PC12 Cells Culture

PC12 cells, rat pheochromocytoma-derived cell line (ATCC CRL-1721) (passages 12–25) were maintained at 37 °C humidified air containing 5% CO₂/95% atmospheric air and cultured in a 60 mm plastic culture plates with Dulbecco's modified Eagle's medium supplemented with 10% horse serum, 5% fetal bovine serum and 1% of penicillin/streptomycin. PC12 cells were treated for 24 h with the different compounds at different concentrations ranging from 1 to 40 μM, to evaluate their eventual toxicity. Then, in order to assess the eventual compounds' protection properties, PC12 cell treated with hydrogen peroxide (100 μM) in association with increasing concentration of the above-mentioned molecules, from 1 up to 20 μM. For the compounds that had been shown to protect cells from the oxidative insult from H₂O₂, a co-treatment with MnCl₂ 1 mM and the compounds was performed, in order to evaluate whether the same compound could also be able to protect against MnCl₂ insult. For all treatments cell viability was measured by means of MTT assay, as explained in the following paragraph [17].

MTT Assay

At the end of the exposure time of each experiment, the cell viability was assessed by means of MTT (3-(4,5-dimethyl-thiazol-2-yl)-2,5-diphenyltetrazoliumbromide) assay. For this purpose, 1 mg/mL of MTT was added to each sample and incubated for 4 h at 37 °C. Only viable cells are able to convert the soluble dye MTT into the insoluble formazan crystals. After the incubation the MTT supernatant solution was removed, the cells were washed in phosphate-buffered saline (PBS) and centrifuged while the pellet was dissolved in 2 mL of isopropanol. After centrifugation of the solution at 4,000 rpm for 5 min, the absorbance for each sample was assessed by means of a Bauty Diagnostic Microplate Reader at 578 nm. All experiments were performed in 24-well plates (1 × 10⁵ cells/mL/well) and repeated in triplicate.

Table S1. Kinetic parameters (V_{MAX} and K_M values) obtained from biosensors' calibrations, without and with the inhibitor. For each inhibitor was built a group of biosensors ($n=4$) for both tyrosinase (TYR) and laccase (LAC) enzyme and parameters' variations were reported. Statistical significance ($p<0.05$) was evaluate by means of t-test.

INHIBITOR	ENZYME	SUBSTRATE (DA)		SUBSTRATE + INHIBITOR	
		V_{MAX} (nA)	K_M (mM)	V_{MAX} (nA)	K_M (mM)
7	TYR	127.2±9.9	0.430±0.181	114.1±12.5	20.030±7.262*
	LAC	218.9±7.1	2.292±0.363	188.4±9.0	17.840±2.907*
8	TYR	47.6±2.2	1.370±0.322	35.2±1.0*	5.769±0.719*
	LAC	99.3±11.3	6.156±1.006	78.7±8.8	9.292±1.677*
9	TYR	224.4±21.6	1.646±0.612	183.2±11.1	9.158±1.762*
	LAC	119.9±9.6	8.658±2.728	90.5±7.4	14.340±4.170*
10	TYR	59.6±3.2	1.334±0.366	31.5±2.9*	7.136±2.729*
	LAC	107.7±12.0	9.400±1.489	89.2±7.7	12.700±1.327*
11	TYR	49.9±1.6	0.596±0.079	33.0±1.1	8.757±1.178*
	LAC	107.7±6.7	7.716±1.932	91.0±9.2*	24.450±7.731*
12	TYR	80.9±3.2	9.330±1.900	63.0±1.962*	11.050±1.409
	LAC	65.1±1.9	4.338±0.741	49.5±6.1	9.640±0.549*
13	TYR	66.9 ±2.0	4.489±0.821	37.3 ±4.0*	9.950±1.284*
	LAC	147.6±21.9	4.727±0.634	114.4±9.5	10.450±1.423*
14	TYR	69.6±3.3	0.504±0.139	48.8±4.67*	7.886±3.033*
	LAC	133.5±3.3	3.667±0.369	110.9±2.4*	7.405±0.578*
15	TYR	83.4±3.5	0.975±0.180	54.3±2.6	9.172±1.714*
	LAC	103.8±3.5	4.439±0.582	93.8±2.9	9.177±0.564*
16	TYR	38.1±3.4	0.569±0.217	22.2±0.6	10.010±1.002*
	LAC	151.5±10.7	6.390±1.655	139.9±6.4	9.933±1.741*
17	TYR	122.4±7.2	1.334±0.366	73.7±26*	7.136±2.729*
	LAC	115.9±13.23	9.304±0.503	96.5±8.3	12.600±0.559*
18	TYR	194.5±14.9	2.851±0.708	145.8±17.8	11.990±3.294*
	LAC	120.1±7.2	5.894±1.505	98.1±3.3	12.380±1.512*
19	TYR	285.6±10.4	7.399±0.688	123.5±9.8*	9.148±1.599
	LAC	124.5±11.1	3.654±1.489	111.4±8.9	7.204±2.640*
20	TYR	87.9±6.0	6.700±0.770	77.4±4.3	11.500±1.142*
	LAC	166.2±12.5	4.182±1.415	151.6±12.1	8.822±2.776*

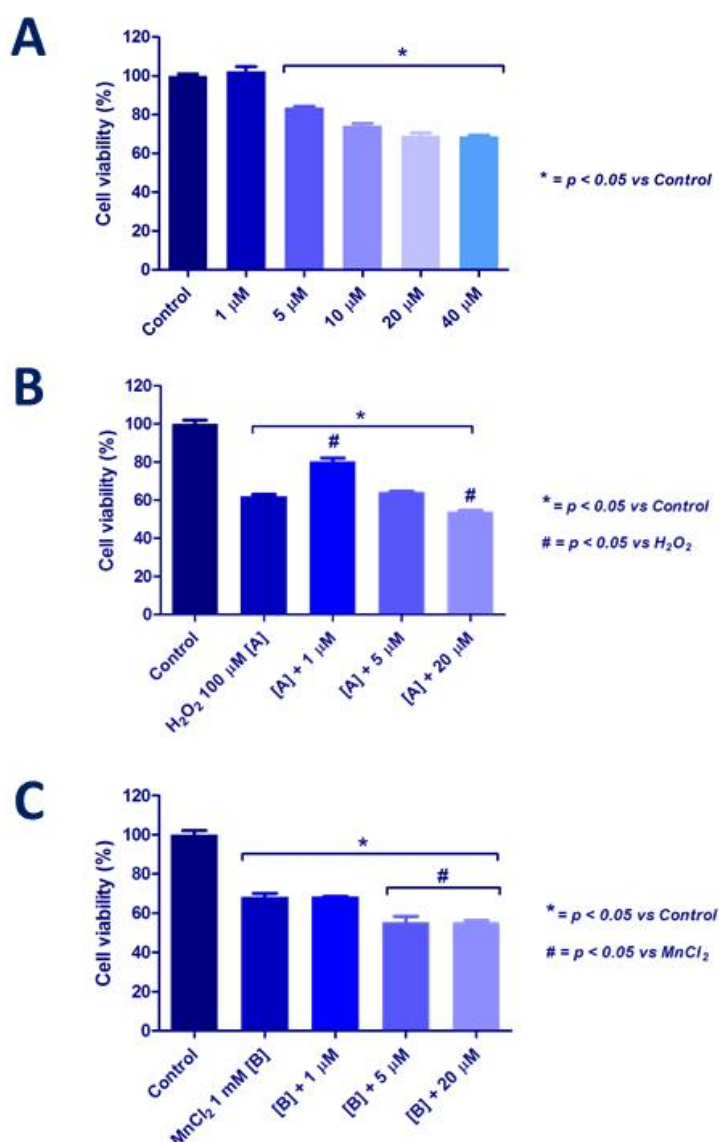
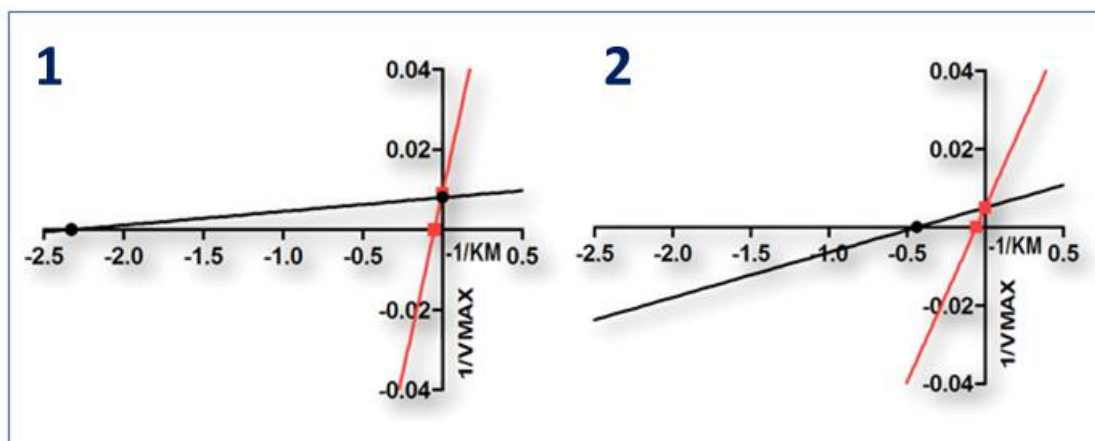


Figure S3: Lineweaver–Burk plot for compound 7 on tyrosinase (inset, 1) and laccase (inset, 2) enzymes. Black line: not inhibited enzyme; red line: inhibited enzyme. Panel A describes the effect of different concentrations of compound 7, ranging from 1 up to 40 μM , on viability of PC12 cells; Panel B and C show the study of potential protective effects of compound 7 on damage induced by H_2O_2 (100 μM) or MnCl_2 (1 mM). MTT assay was performed on PC12 cells 24 h after each treatment. * $p < 0.05$ vs control; # $p < 0.05$ vs H_2O_2 or MnCl_2

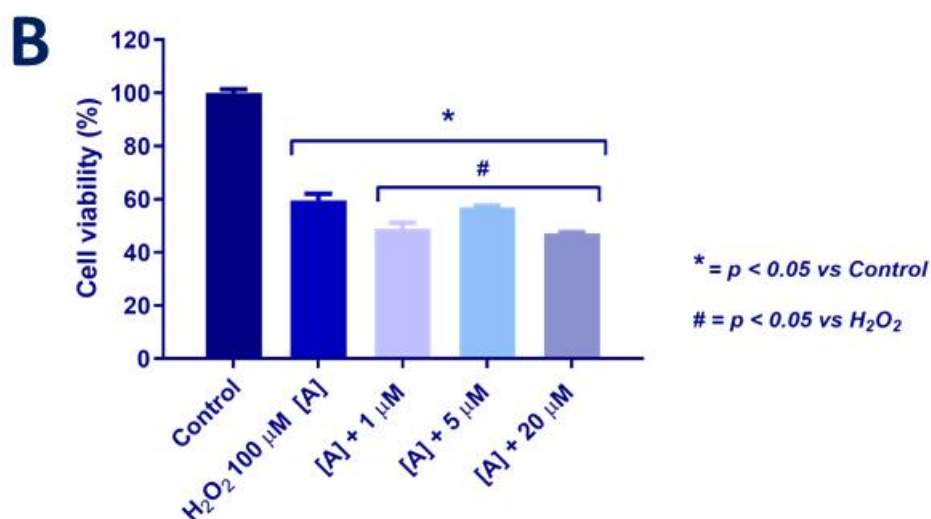
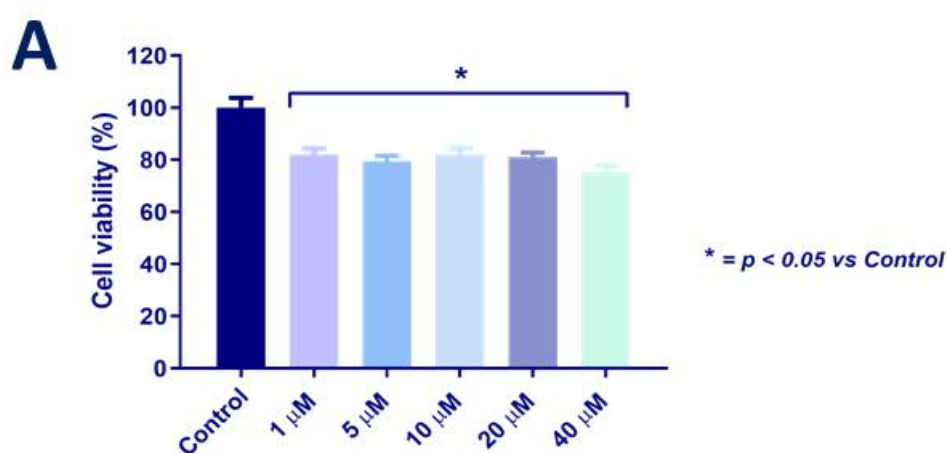
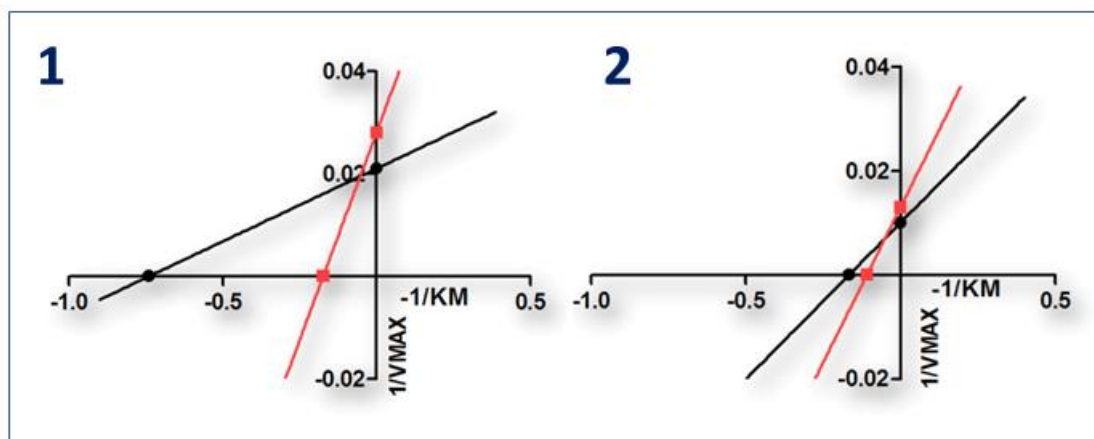


Figure S4: Lineweaver–Burk plot for compound 8 on tyrosinase (inset, 1) and laccase (inset, 2) enzymes. Black line: not inhibited enzyme; red line: inhibited enzyme. Panel A describes the effect of different concentrations of compound 8, ranging from 1 up to 40 μM , on viability of PC12 cells; Panel B shows the study of potential protective effects of compound 8 on damage induced by H₂O₂ (100 μM). MTT assay was performed on PC12 cells 24 h after each treatment. * $p < 0.05$ vs control; # $p < 0.05$ vs H₂O₂

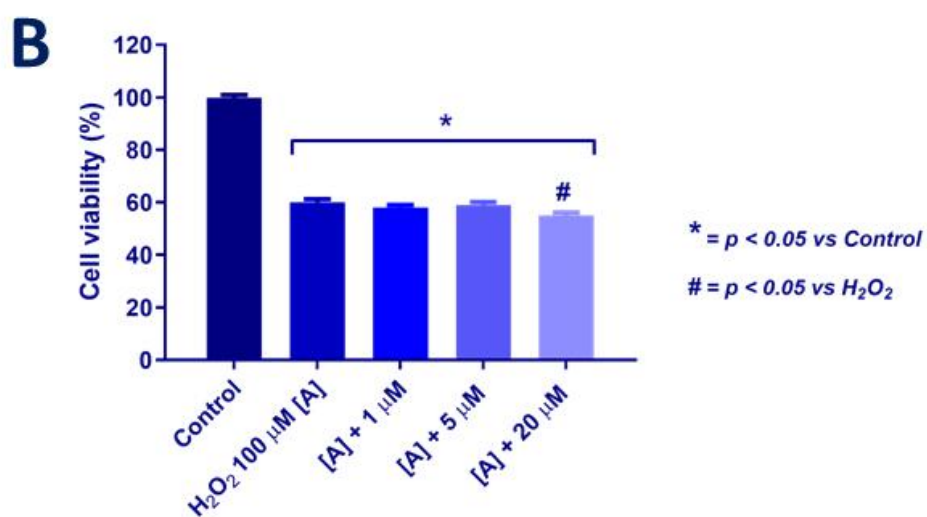
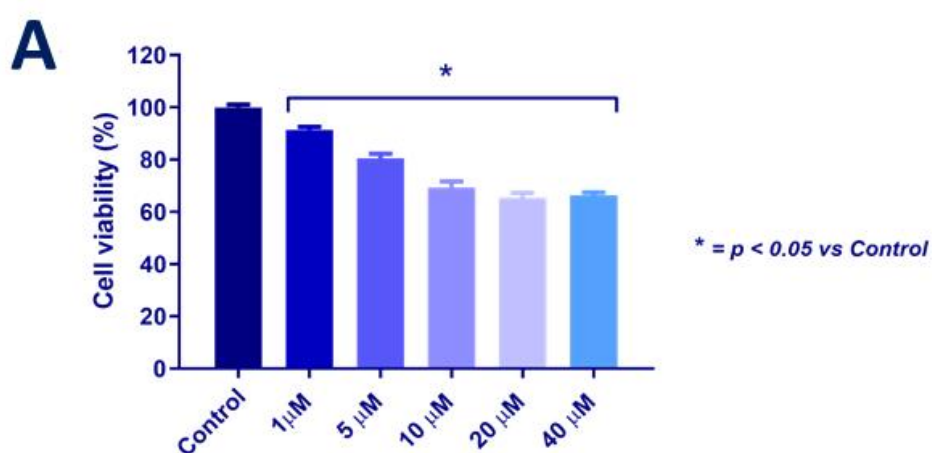
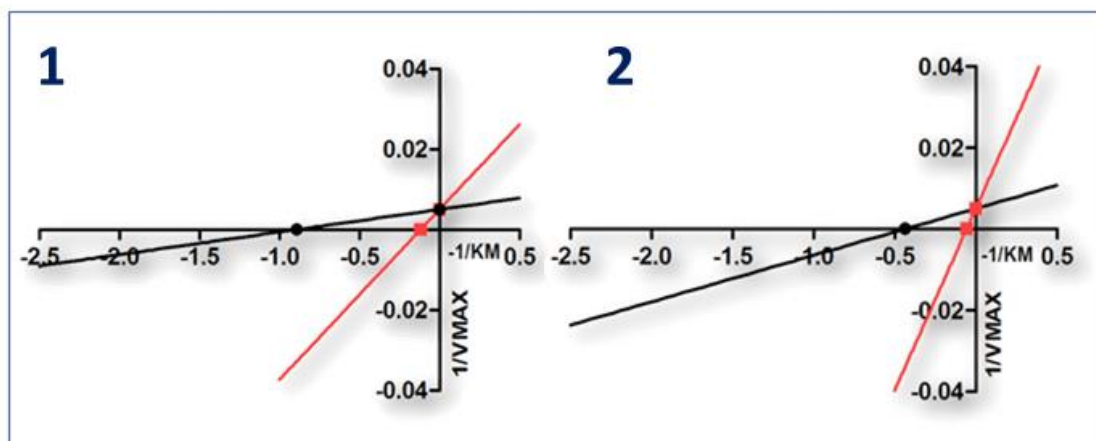


Figure S5: Lineweaver–Burk plot for compound 9 on tyrosinase (inset, 1) and laccase (inset, 2) enzymes. Black line: not inhibited enzyme; red line: inhibited enzyme. Panel A describes the effect of different concentrations of compound 9, ranging from 1 up to 40 μM, on viability of PC12 cells; Panel B shows the study of potential protective effects of compound 9 on damage induced by H₂O₂ (100 μM). MTT assay was performed on PC12 cells 24 h after each treatment. * $p < 0.05$ vs control; # $p < 0.05$ vs H₂O₂.

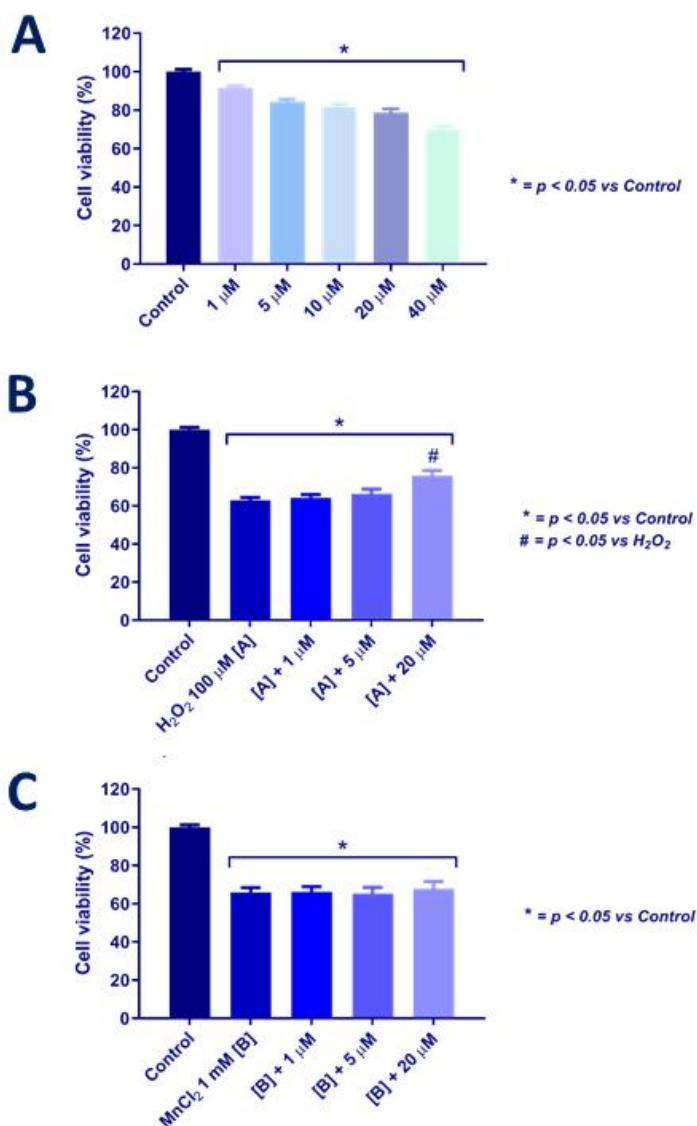
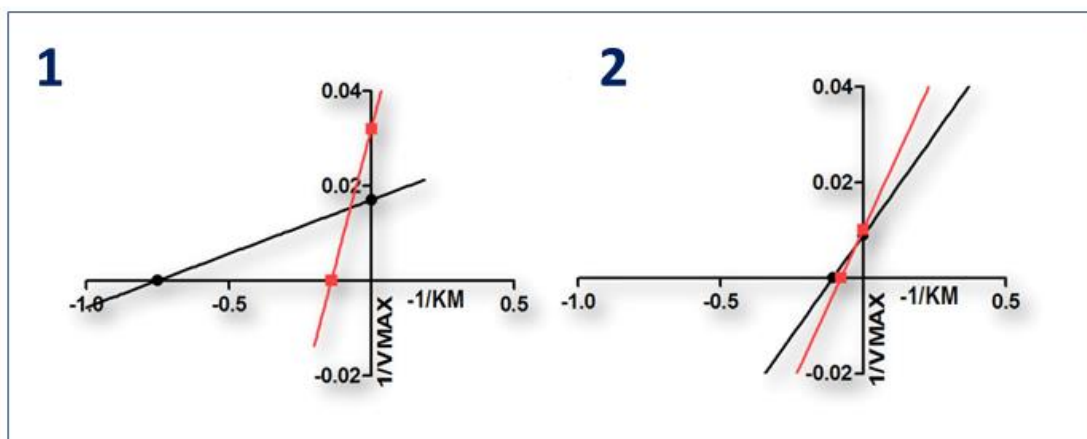


Figure S6: Lineweaver–Burk plot for compound **10** on tyrosinase (inset, 1) and laccase (inset, 2) enzymes. Black line: not inhibited enzyme; red line: inhibited enzyme. Panel A describes the effect of different concentrations of compound **10**, ranging from 1 up to 40 μ M, on viability of PC12 cells; Panel B and C show the study of potential protective effects of compound **10** on damage induced by H_2O_2 (100 μ M) or $MnCl_2$ (1 mM). MTT assay was performed on PC12 cells 24 h after each treatment. * $p < 0.05$ vs control; # $p < 0.05$ vs H_2O_2 or $MnCl_2$

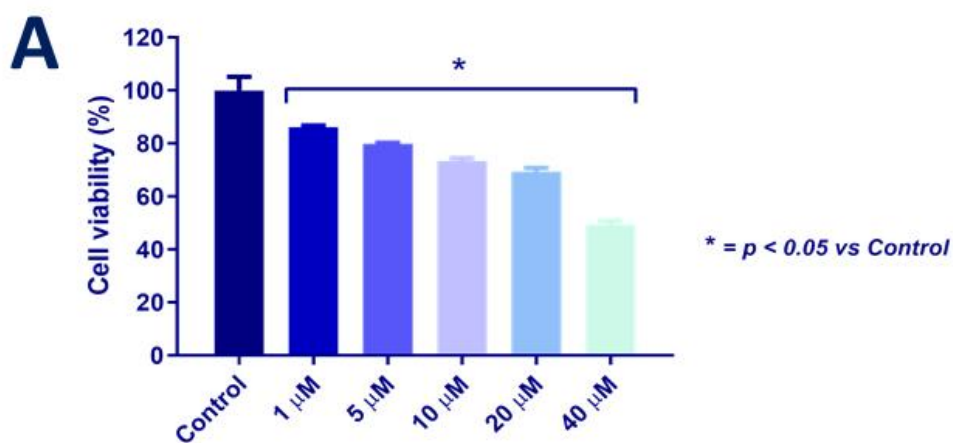
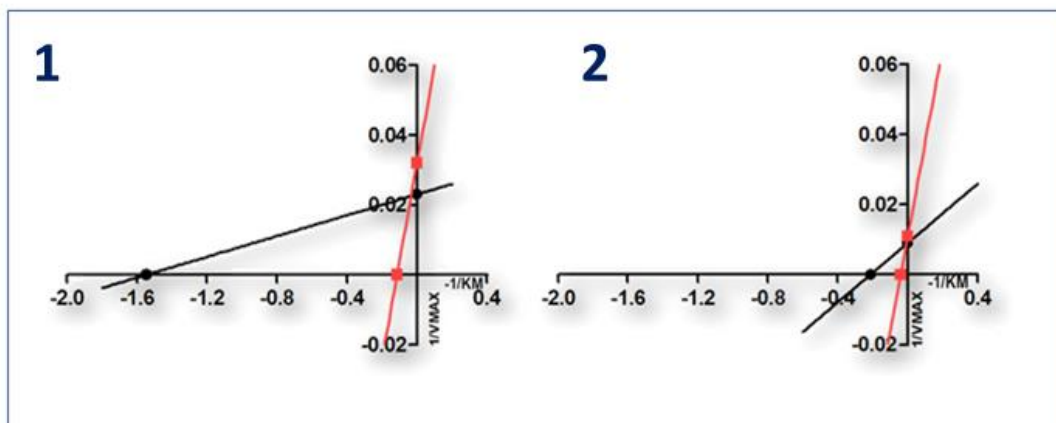


Figure S7: Lineweaver–Burk plot for compound 11 on tyrosinase (inset, 1) and laccase (inset, 2) enzymes. Black line: not inhibited enzyme; red line: inhibited enzyme. Panel A describes the effect of different concentrations of compound 11, ranging from 1 up to 40 μM , on viability of PC12 cells. MTT assay was performed on PC12 cells 24 h after each treatment. * $p < 0.05$ vs control.

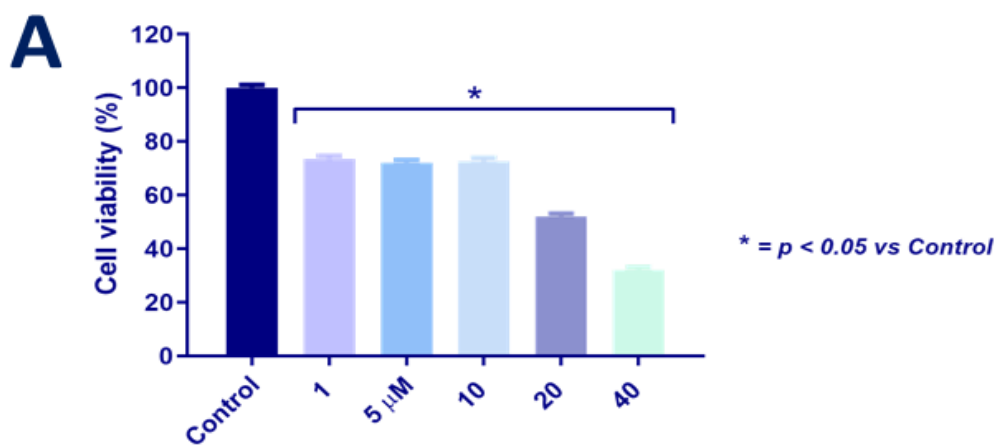
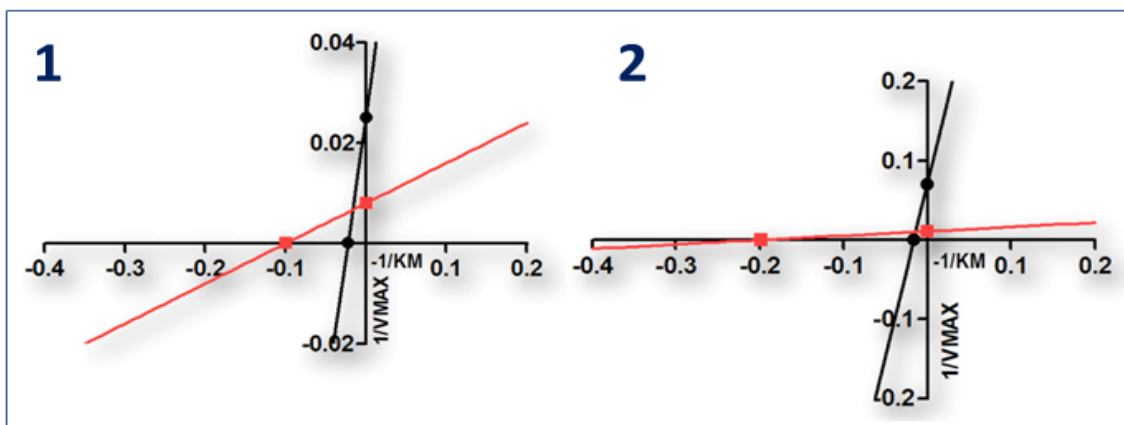


Figure S8: Lineweaver–Burk plot for compound **12** on tyrosinase (inset, 1) and laccase (inset, 2) enzymes. Black line: not inhibited enzyme; red line: inhibited enzyme. Panel A describes the effect of different concentrations of compound **12**, ranging from 1 up to 40 μ M, on viability of PC12 cells. MTT assay was performed on PC12 cells 24 h after each treatment. * $p < 0.05$ vs control.

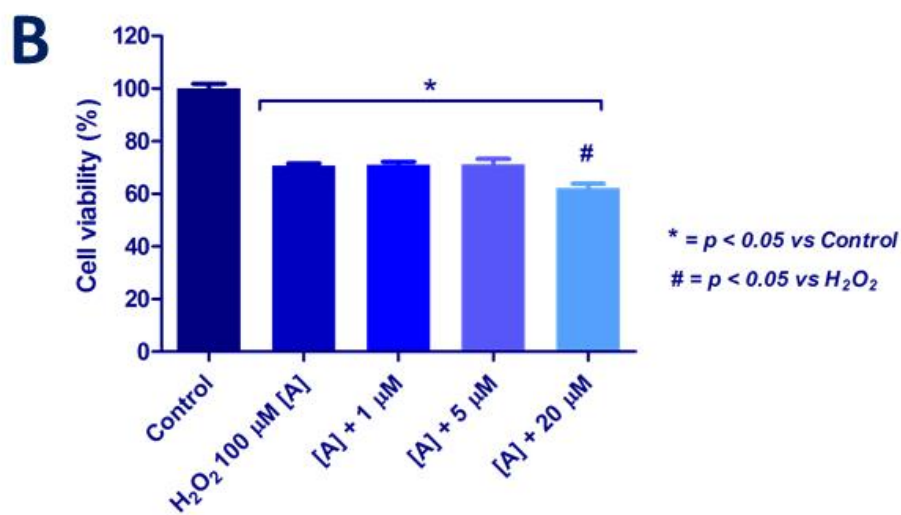
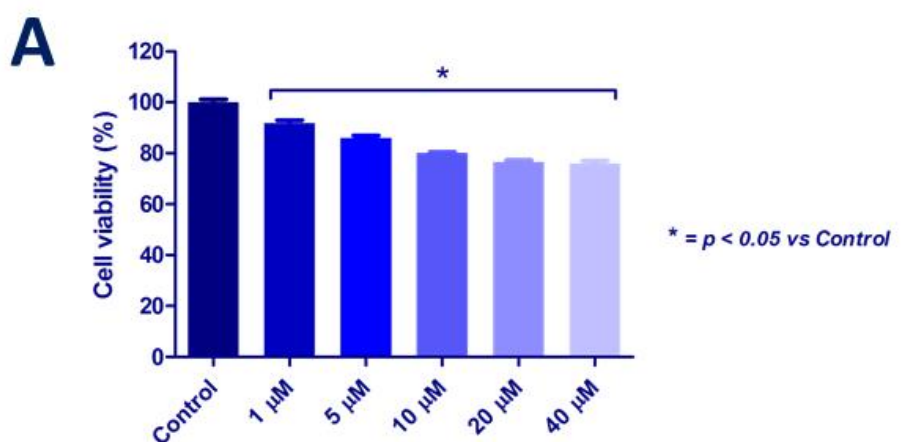
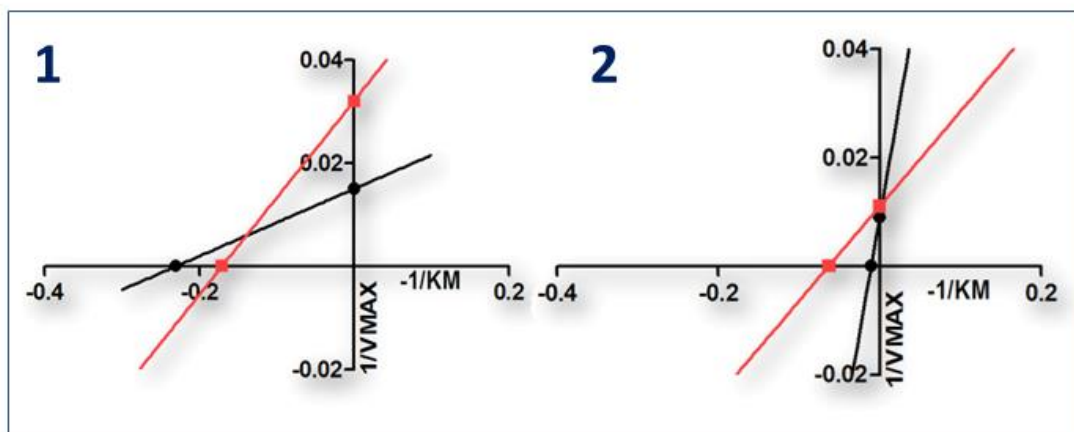


Figure S9: Lineweaver–Burk plot for compound 13 on tyrosinase (inset, 1) and laccase (inset, 2) enzymes. Black line: not inhibited enzyme; red line: inhibited enzyme. Panel A describes the effect of different concentrations of compound 13, ranging from 1 up to 40 μM , on viability of PC12 cells; Panel B shows the study of potential protective effects of compound 13 on damage induced by H_2O_2 (100 μM). MTT assay was performed on PC12 cells 24 h after each treatment. $*p < 0.05$ vs control; $\#p < 0.05$ vs H_2O_2 .

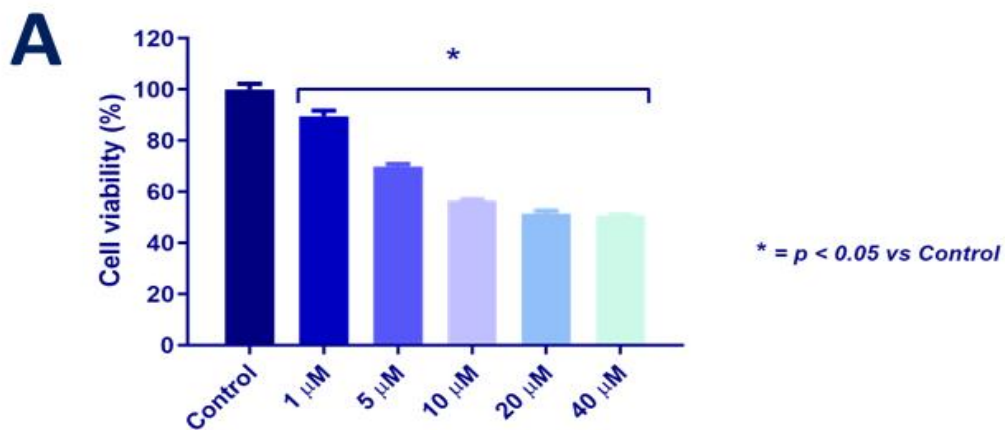
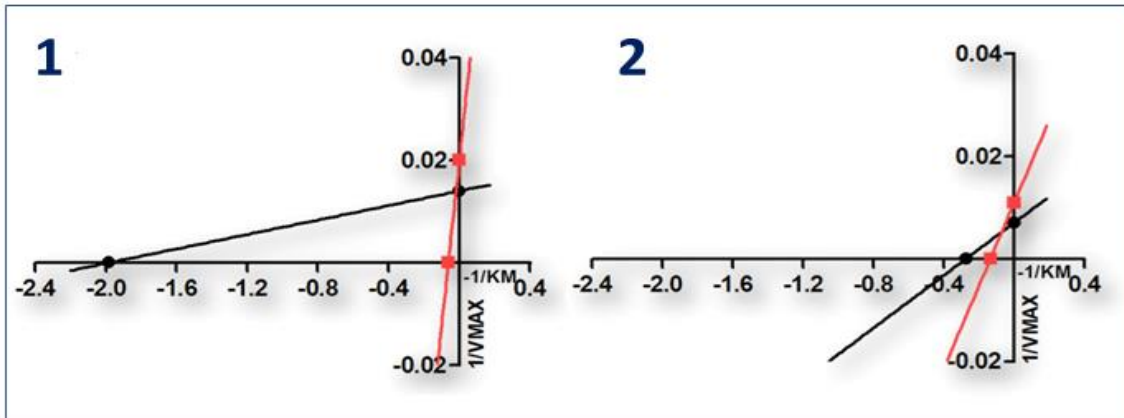


Figure S10: Lineweaver-Burk plot for compound 14 on tyrosinase (inset, 1) and laccase (inset, 2) enzymes. Black line: not inhibited enzyme; red line: inhibited enzyme. Panel A describes the effect of different concentrations of compound 14, ranging from 1 up to 40 μM , on viability of PC12 cells. MTT assay was performed on PC12 cells 24 h after each treatment. * $p < 0.05$ vs control.

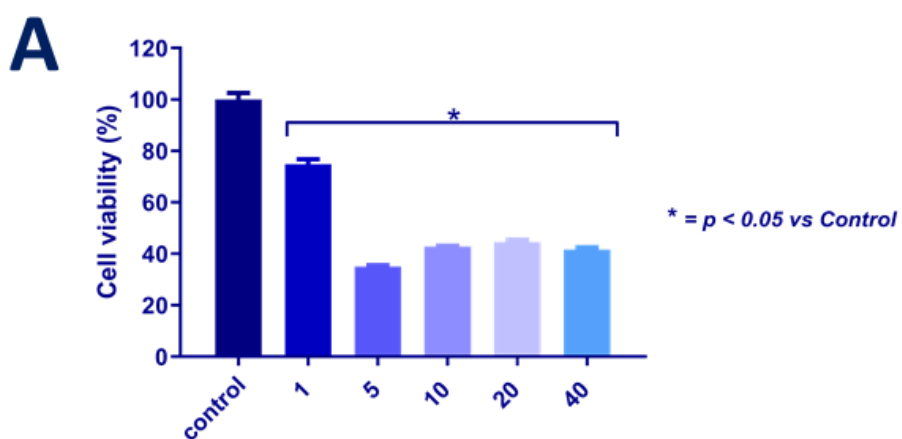
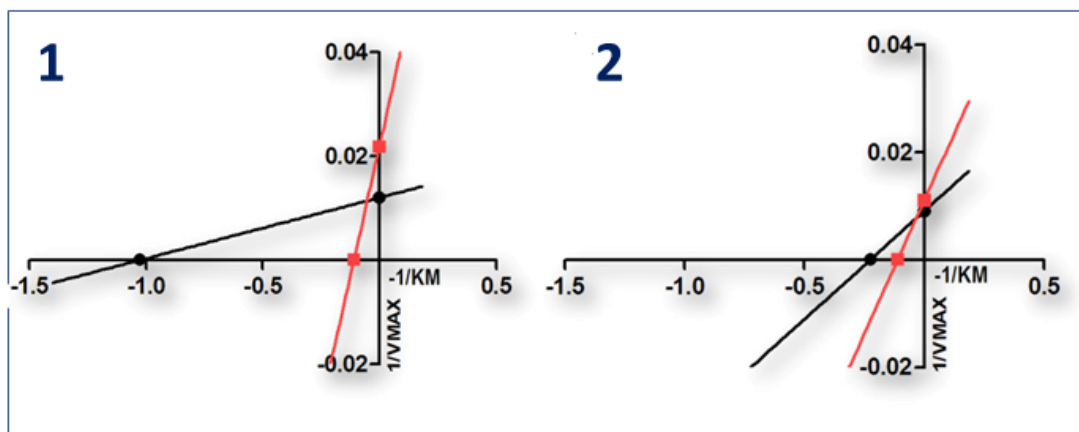


Figure S11: Lineweaver–Burk plot for compound **15** on tyrosinase (inset, 1) and laccase (inset, 2) enzymes. Black line: not inhibited enzyme; red line: inhibited enzyme. Panel A describes the effect of different concentrations of compound **15**, ranging from 1 up to 40 μM , on viability of PC12 cells. MTT assay was performed on PC12 cells 24 h after each treatment. * $p < 0.05$ vs control.

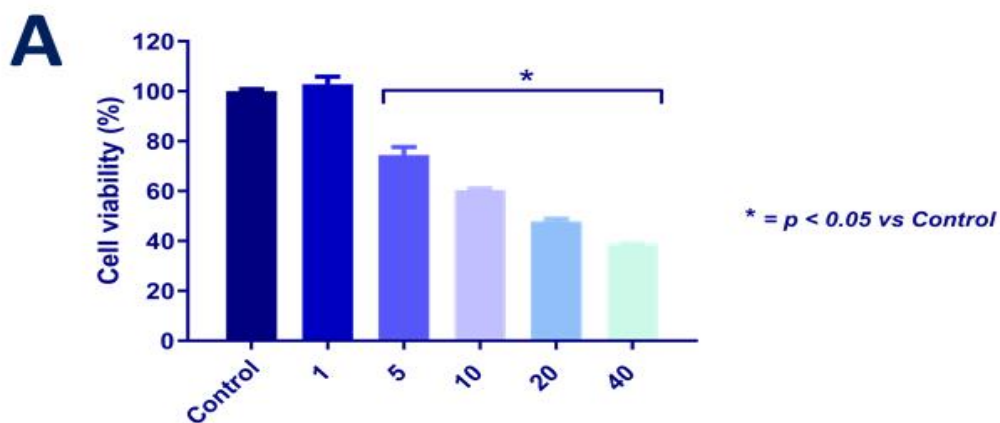
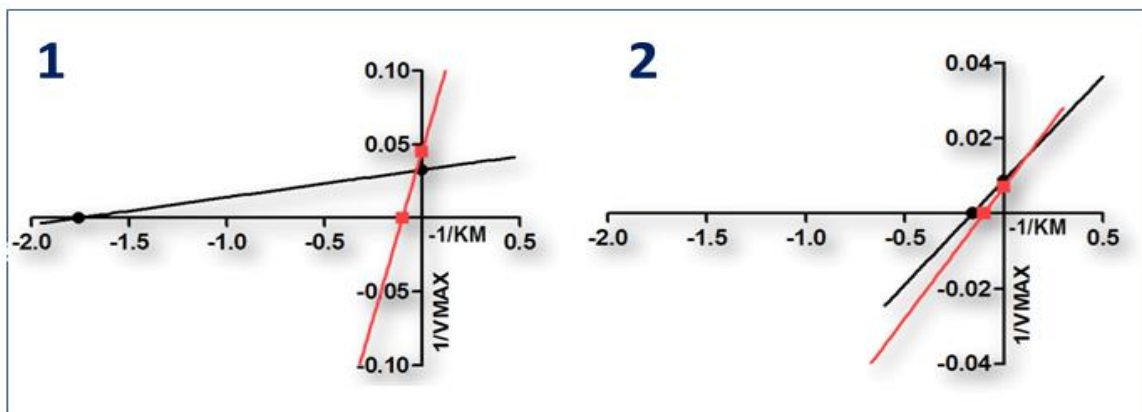


Figure S12: Lineweaver–Burk plot for compound **16** on tyrosinase (inset, 1) and laccase (inset, 2) enzymes. Black line: not inhibited enzyme; red line: inhibited enzyme. Panel A describes the effect of different concentrations of compound **16**, ranging from 1 up to 40 μM , on viability of PC12 cells. MTT assay was performed on PC12 cells 24 h after each treatment. * $p < 0.05$ vs control.

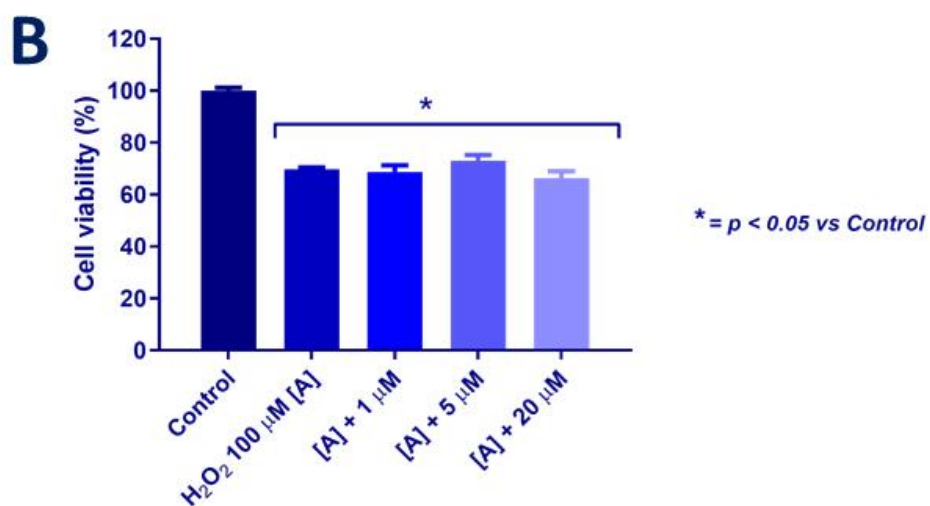
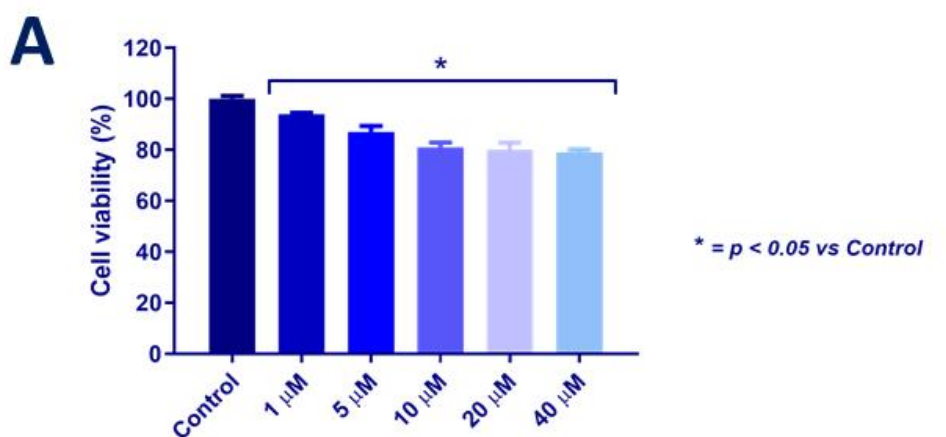
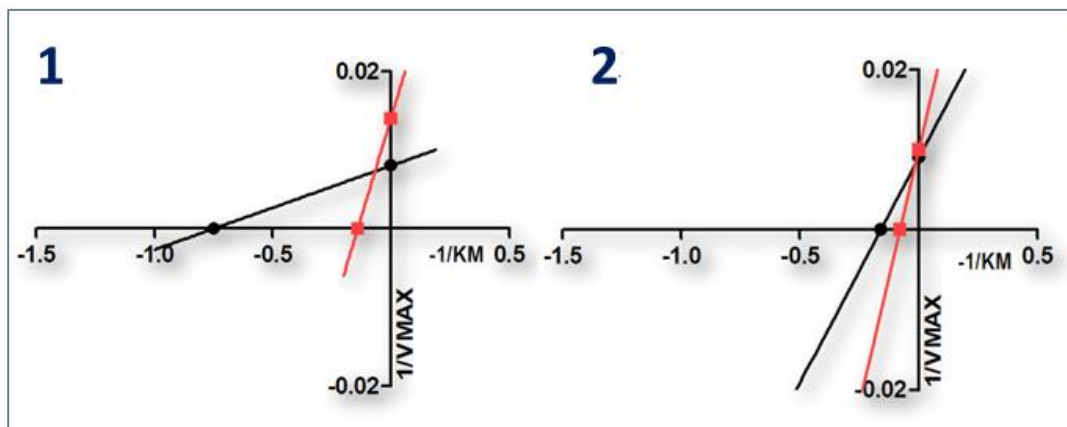


Figure S13: Lineweaver–Burk plot for compound 17 on tyrosinase (inset, 1) and laccase (inset, 2) enzymes. Black line: not inhibited enzyme; red line: inhibited enzyme. Panel A describes the effect of different concentrations of compound 17, ranging from 1 up to 40 μM , on viability of PC12 cells; Panel B shows the study of potential protective effects of compound 17 on damage induced by H₂O₂ (100 μM). MTT assay was performed on PC12 cells 24 h after each treatment. * $p < 0.05$ vs control.

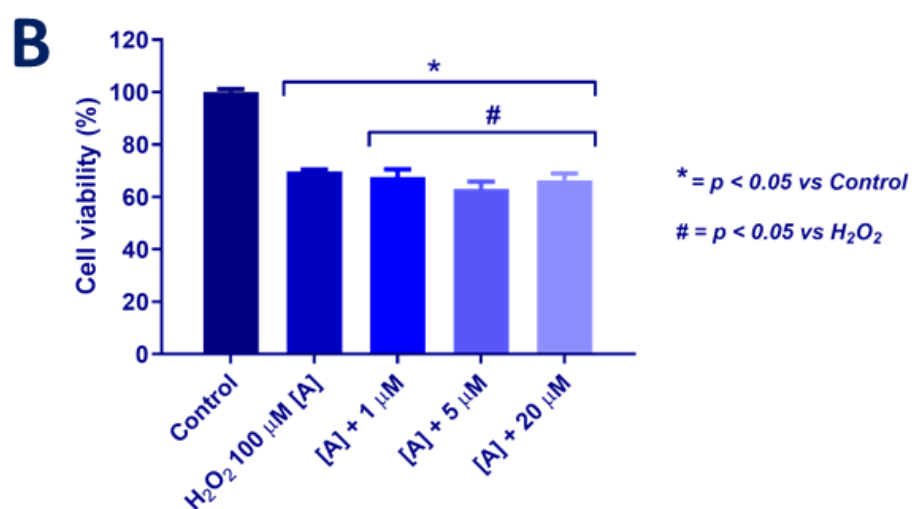
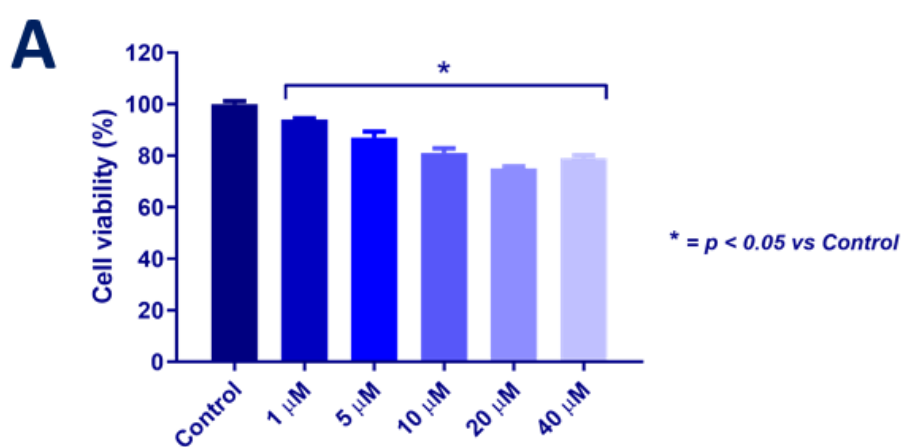
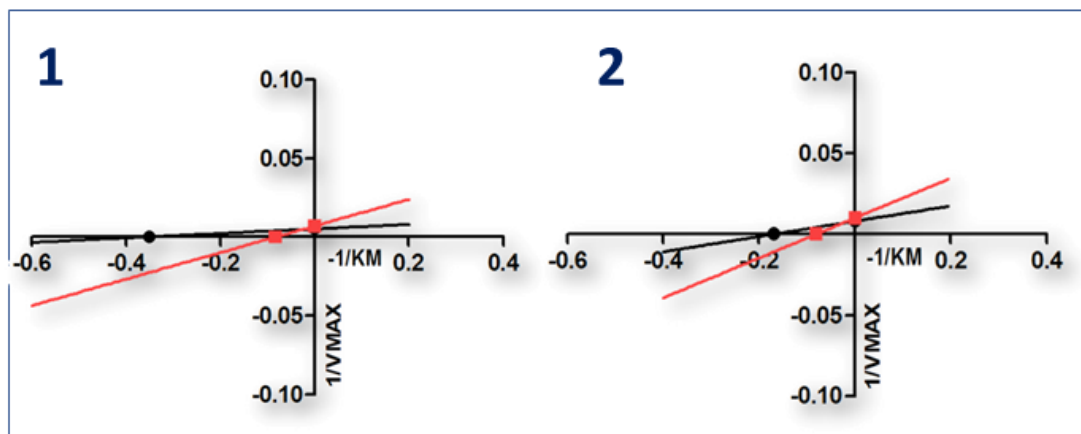


Figure S14: Lineweaver–Burk plot for compound **18** on tyrosinase (inset, 1) and laccase (inset, 2) enzymes. Black line: not inhibited enzyme; red line: inhibited enzyme. Panel A describes the effect of different concentrations of compound **18**, ranging from 1 up to 40 μM , on viability of PC12 cells; Panel B shows the study of potential protective effects of compound **18** on damage induced by H₂O₂ (100 μM). MTT assay was performed on PC12 cells 24 h after each treatment. * $p < 0.05$ vs control.

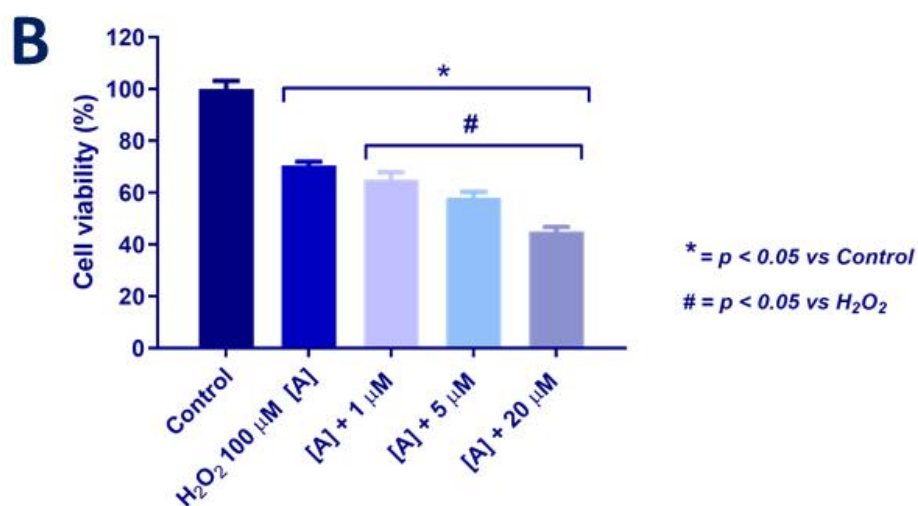
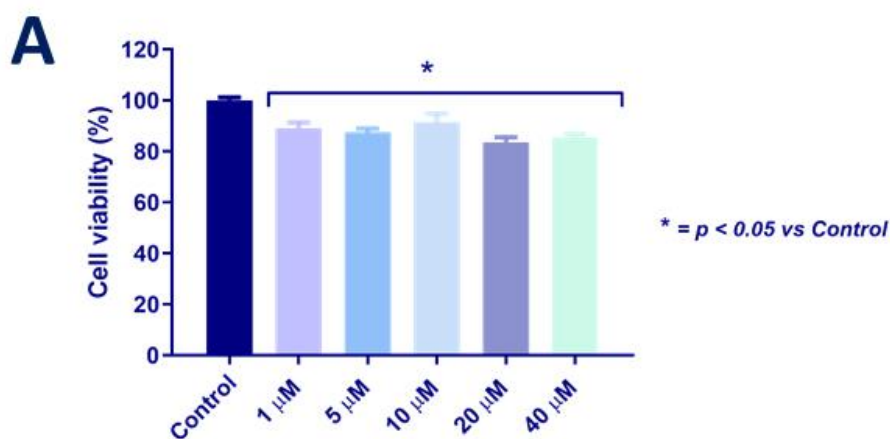
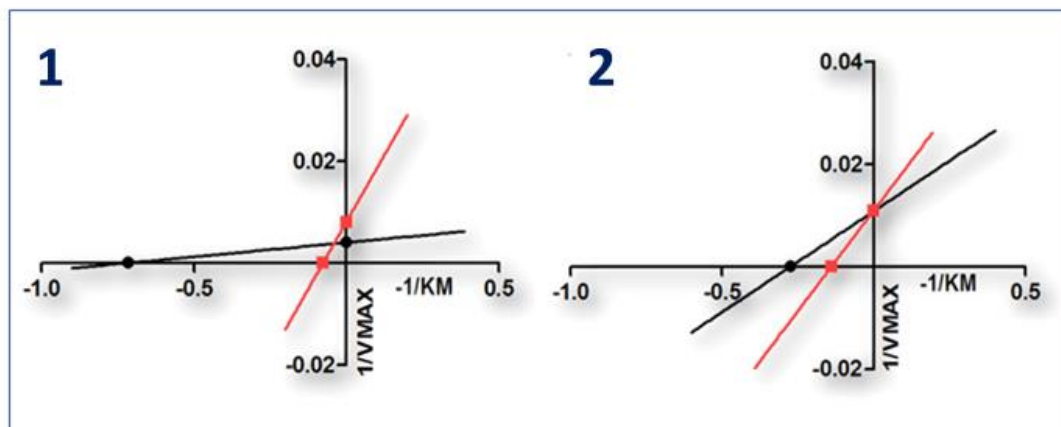


Figure S15: Lineweaver–Burk plot for compound **19** on tyrosinase (inset, 1) and laccase (inset, 2) enzymes. Black line: not inhibited enzyme; red line: inhibited enzyme. Panel A describes the effect of different concentrations of compound **19**, ranging from 1 up to 40 μ M, on viability of PC12 cells; Panel B and C show the study of potential protective effects of compound **19** on damage induced by H_2O_2 (100 μ M). MTT assay was performed on PC12 cells 24 h after each treatment. * $p < 0.05$ vs control.

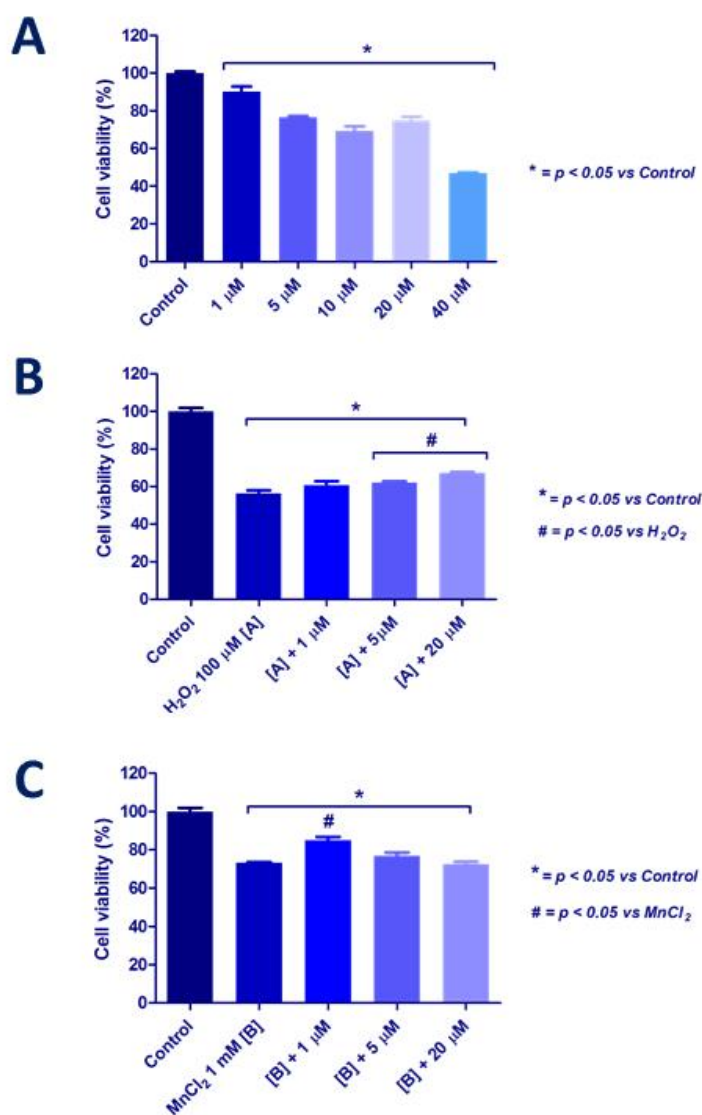
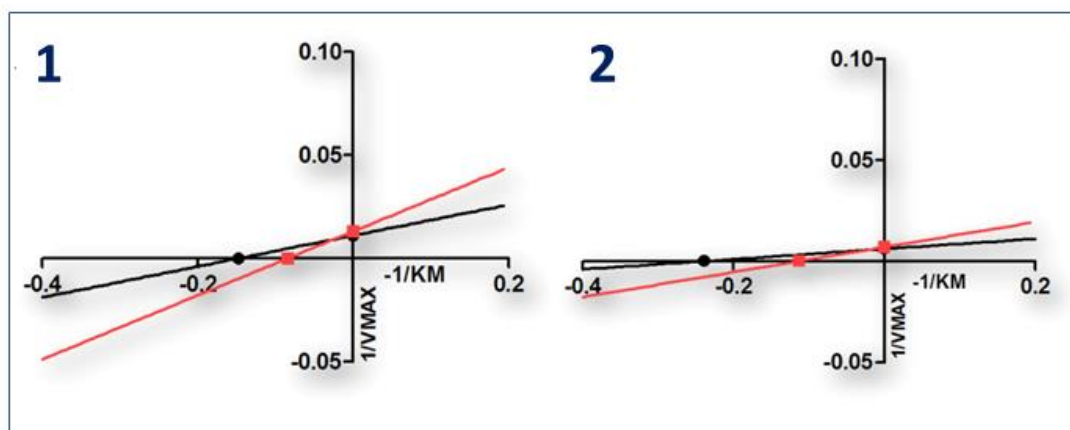


Figure S16: Lineweaver–Burk plot for compound **20** on tyrosinase (inset, 1) and laccase (inset, 2) enzymes. Black line: not inhibited enzyme; red line: inhibited enzyme. Panel A describes the effect of different concentrations of compound **20**, ranging from 1 up to 40 μM , on viability of PC12 cells; Panel B and C show the study of potential protective effects of compound **20** on damage induced by H₂O₂ (100 μM) or MnCl₂ (1 mM). MTT assay was performed on PC12 cells 24 h after each treatment. * $p < 0.05$ vs control; # $p < 0.05$ vs H₂O₂ or MnCl₂

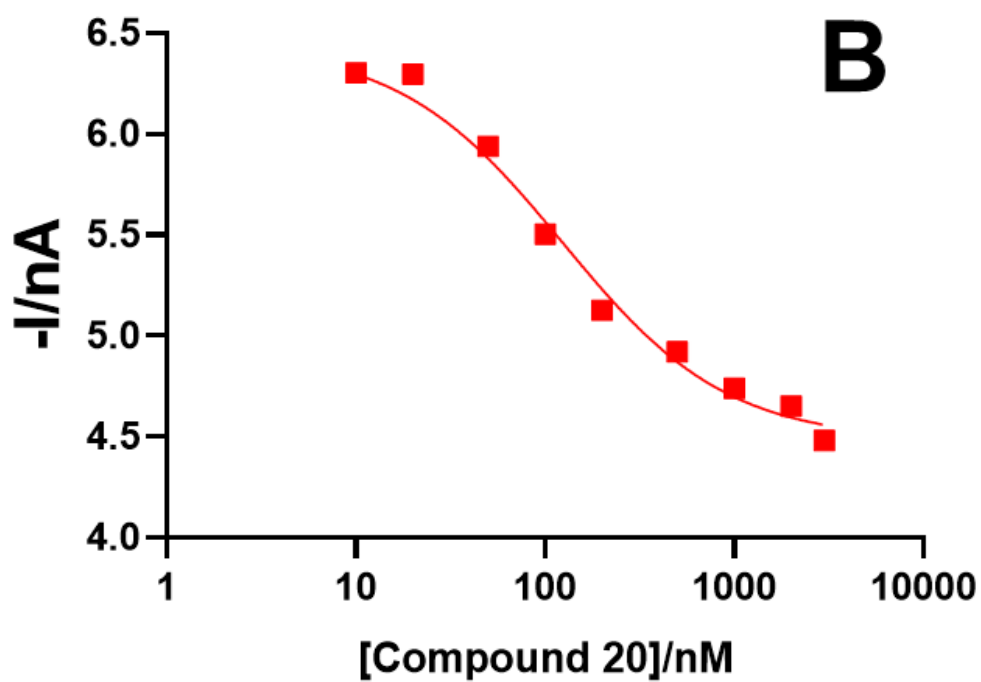
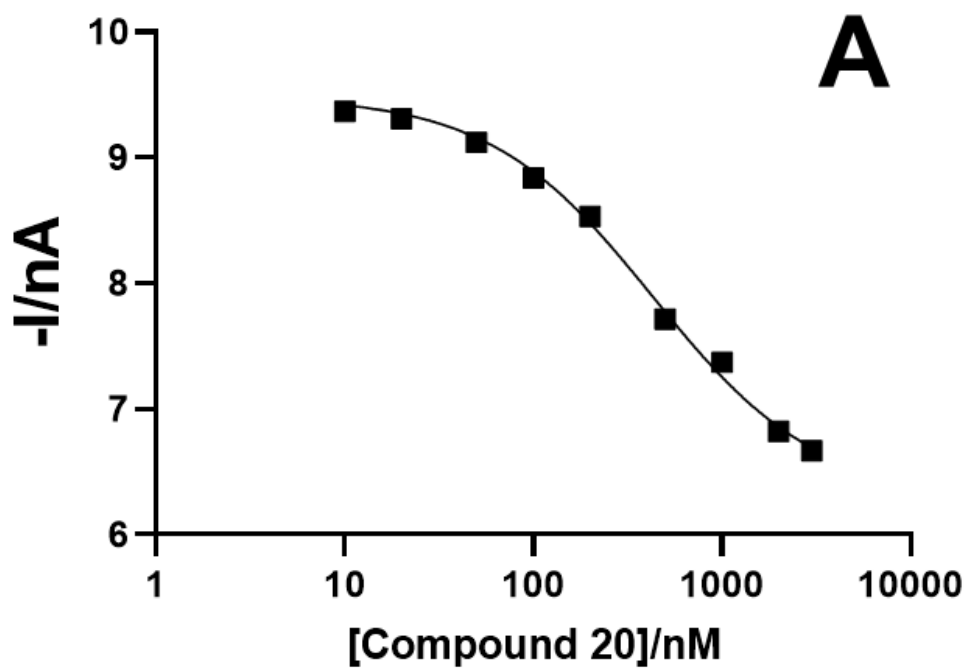


Figure S17: Representative plot of IC_{50} calculation for compound 20. In panel A is reported the inhibition effect of the studied molecule on tyrosinase enzyme ($IC_{50} = 422.7$ nM; $R^2 = 0.996$), while in panel B is shown the inhibition on laccase enzyme ($IC_{50} = 117.8$ nM; $R^2 = 0.991$). Both enzymes were immobilized on the biosensor surface.

1.6 Computational studies

Table S2. Estimated interactions of compounds **DFB**, **1** and **20** with the residue of amino acids of Cu1 T1 site of laccase

Ligand	% Cluster ^a	focc ^b	M.B.E. ^c	E.F.E.B. ^d	E.I.C., <i>K_i</i> ^e	Interaction with amino acids, H-Bonds
DFB	69	3/3	-5.68	-5,79	56.87 μ M	PHE162 PRO163 ASP206 ASN264 PHE265 GLY392 ALA393 PRO394 ILE455 HIS458
1	100	1/1	-5.38	-5,41	108.39 μ M	PHE162 PRO163 ASP206 ASN264 PHE265 GLY392 ALA393 PRO394 ILE455 HIS458
20	25	23/14	-5.58	-6,18	29.54 μ M	PHE162 PRO163 LEU164 ASP206 ASN264(2) PHE265 GLY266 GLY392 ALA393 ILE455 HIS458

^a % Cluster: percentage number of similar conformation grouped by rmsd-tolerance of 2.0 angstrom,

^b focc: n° of distinct conformational clusters/n° of multi-member conformational clusters, out of 100 runs, using an rmsd-tolerance of 2.0 angstrom,

^c M.B.E.: Mean Binding Energy,

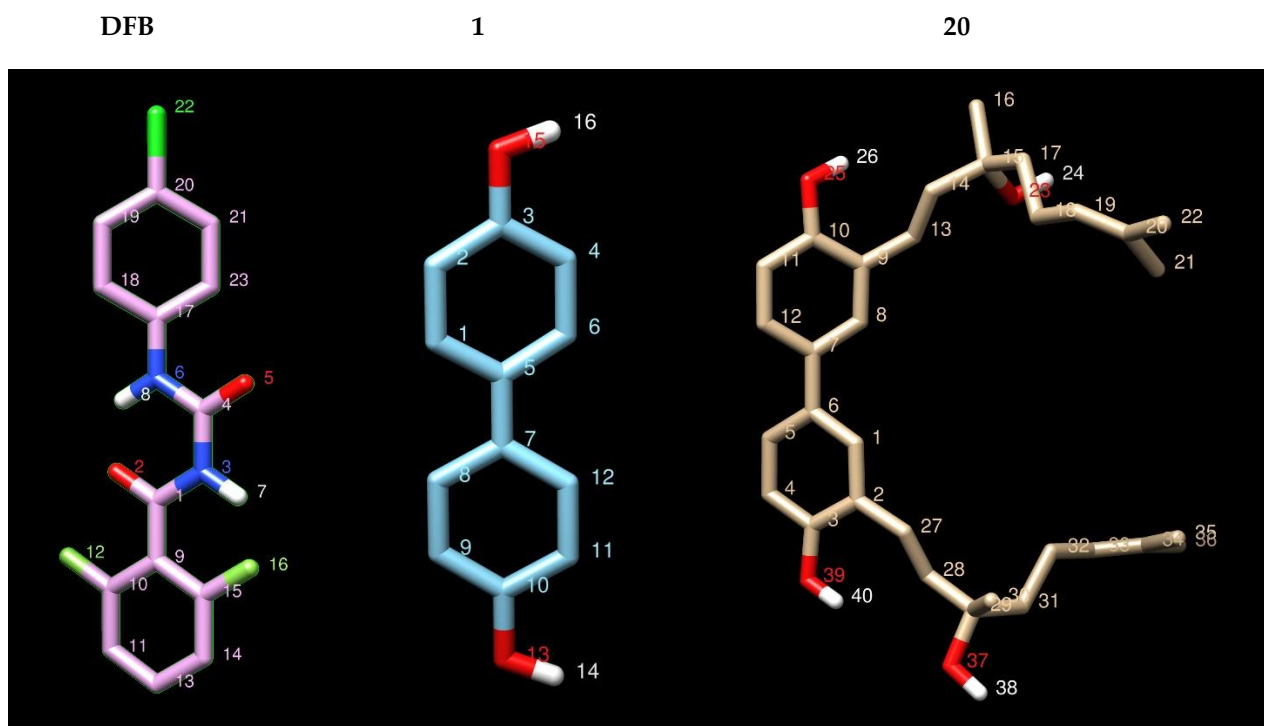
^d E.F.E.B.: Estimated Free Energy of Binding,

^e E.I.C.,*K_i*: Estimated Inhibition Constant, *K_i*,

Table S3. Estimated H-bonds of compounds **DFB**, **1** and **20** with the residue of amino acids of Cu1 T1 site of laccase

Ligands	H-bond	Ligands Atom	Protein Atom	Distance (Å)	Ang. °
DFB	1	H7(HD) ^a	ALA393:O(OA) ^b	2,237	132,97
1	2	H16(HD)	PRO163:O(OA)	2,126	153,42
		H14(HD)	ALA393:O(OA)	1,803	129,86
20	3	H40(HD)	PHE162:O(OA)	1,757	146,24
		H24(HD)	ASN264:OD1(OA)	2,021	159,14
		H26(HD)	ASN264:OD1(OA)	2,153	155,25

^a (HD) hydrogen donors, ^b (OA) oxygen acceptors



1.7 References

1. Marchiani, A.; Mammi, S.; Siligardi, G.; Hussain, R.; Tessari, I.; Bubacco, L.; Delogu, G.; Fabbri, D.; Dettori, M. A.; Sanna, D.; Dedola, S.; Serra, P.A.; Ruzza, P. Small molecules interacting with α -synuclein: antiaggregating and cytoprotective properties. *Amino Acids* **2013**, *45*, 327-338.
2. Baranovsky, A.; Schmitt, B.; Fowler, J.D.; Schneider, B. *Synth. Commun.* 2006, 1019-1045; b) Chuprajob, T.; Chatchawan, C.; Chokchaisiric, R.; Chunglok, W.; Sornkaewa, N.; Apichart Suksamrarna, A. Synthesis, cytotoxicity against human oral cancer KB cells and structure–activity relationship studies of trienone analogues of curcuminoids. *Bioorg. Med. Chem. Lett.*, **2014**, *24*, 2839-2844.
3. Jae-Chul, J.; Soyong, J.; Yongam, L.; Dongguk, M.; Eunyong, L.; Heyin, J.; Miyeon, O.; Seikwan, O.; Mankil, J. Efficient synthesis and neuroprotective effect of substituted 1,3-diphenyl-2-propen-1-ones. *J. Med. Chem.* **2008**, *51*, 4054–4058.
4. Pathak, V.; Ahmad, I.; Kahlon, A.K.; Hasanian, M.; Sharma, S.; Srivastava, K.K.; Sarkar, J.; Shankar, K.; Gupta, A. Syntheses of 2-methoxyestradiol and eugenol template based diarylpropenes as non-steroidal anticancer agents. *RSC Advances*, **2014**, *4*, 35171-35185.
5. Kuo, P.C.; Damu, A. C.; Cheng, C. Y.; Jeng, J.F.; Teng, C.M.; Lee, E.J.; Wu, T.S. Isolation of a Natural Antioxidant, Dehydrozingerone from *Zingiber officinale* and Synthesis of Its Analogues for Recognition of Effective Antioxidant and Antityrosinase Agents *Arch Pharm Res* **2005**, *28*, 518-528.
6. Ocasio-Malave, C.; Donate, M.J.; Sanchez, M.M.; Sosa-Rivera, J.M.; Mooney, J.W.; Perales-DeLeon, T.A.; Carballera, N.M.; Martinez-Ferrer, M.; Sanabria-Rios, D.J. Synthesis of novel 4-Boc-piperidone chalcones and evaluation of their cytotoxic activity against highly-metastatic cancer cells. *Bioorg. Med. Chem. Lett.* **2020**, *30*, 1, 126760.
7. Delogu, G.; Dettori, M.A.; Patti, A.; Pedotti, S.; Forni, A.; Casalone, G. Stereoselective oxazaborolidine–borane reduction of biphenylalkyl diketones–lignin models: enantiopure dehydrodiapocynol derivatives. *Tetrahedron:Asymmetry*, **2003**, *14*, 2467-2474.
8. Pisano, M.; Pagnan, G.; Dettori, M.A.; Cossu, S.; Caffa, I.; Sassu, I.; Emionite, L.; Fabbri, D.; Cilli, M.; Pastorino, F.; Palmieri, G.; Delogu, G.; Ponzoni, M.; Rozzo, C. Enhanced anti-tumor activity of a new *curcumin*-related compound against melanoma and neuroblastoma cells. *Mol.Cancer*. **2010**, *9*, 137.
9. Russel W.R.; Scobbie, L.; Chesson, A. *Bioorg. & Med. Chem.* Structural modification of phenylpropanoid-derived compounds and the effects on their participation in redox processes. *Bioorg. Med. Chem.* **2005**, *13*, 2537–2546.
10. Bragnier, N.; Guillot, R.; Sherrmann, M.C. Diastereoselective addition of sugar radicals to camphorsultam glyoxilic oxime ether: a route toward C-glycosylthreonine and allothreonine. *Org. Biomol. Chem.* **2009**, *7*, 3918-3921.
11. Calia, G.; Rocchitta, G.; Migheli, R.; Puggioni, G.; Spissu, Y.; Bazzu, G.; Mazzarello, V.; Lowry, J.P.; O'Neill, R.D.; Desole, M.S.; Serra, P.A. Biotelemetric monitoring of brain neurochemistry in conscious rats using microsensors and biosensors. *Sensors (Basel)*. **2009**, *9*, 2511-2523.

12. Bazzu, G.; Puggioni, G.G.; Dedola, S.; Calia, G.; Rocchitta, G.; Migheli, R.; Desole, M.S.; Lowry, J.P.; O'Neill, R.D.; Serra, P.A. Real-time monitoring of brain tissue oxygen using a miniaturized biotelemetric device implanted in freely moving rats. *Anal Chem.* **2009**, *81*, 2235-2241.
13. Rocchitta, G.; Migheli, R.; Dedola, S.; Calia, G.; Desole, M.S.; Miele, E.; Lowry, J.P.; O'Neill, R.D.; Serra, P.A. Development of a distributed, fully automated, bidirectional telemetry system for amperometric microsensor and biosensor applications. *Sens. Actuators B Chem* **2007**, *126*, 700-709.
14. Barberis, A.; Garbetta, A.; Cardinali, A.; Bazzu, G.; D'Antuono, I.; Rocchitta, G.; Fadda, A.; Linsalata, V.; D'Hallewin, G.; Serra, P.A.; Minervini, F. Real-time monitoring of glucose and phenols intestinal absorption through an integrated Caco-2/TC7 cells/biosensors telemetric device: Hypoglycemic effect of fruit phytochemicals. *Biosens Bioelectron.* **2017**, *88*, 159-166.
15. Tamara, H.; Benoît, S.; Stojanc, J.; Weikb, M.; Martyd, J.L; Fourniera, D. Kinetic insight into the mechanism of cholinesterase inhibition by aflatoxin B1 to develop biosensors. *Biosens. Bioelectron.* **2009**, *24*, 2119-2124.
16. Turdean, G.L. Design and development of biosensors for the detection of heavy metal toxicity. *Int. J. Electrochem.* **2011**, Volume 2011, Article ID 343125.
17. Pinna, A.; Ricco, R.; Migheli, R.; Rocchitta, G.; Serra, P.A.; Falcaro, P.; Malfatti, L.; Innocenzi, P. A MOF-based carrier for in situ dopamine delivery, *RSC Advances* **2018**, *8*, 25664-25672.